RESEARCH LETTER –Pathogens & Pathogenicity

Pleiotropic consequences of gene knockouts in the phthiocerol dimycocerosate and phenolic glycolipid biosynthetic gene cluster of the opportunistic human pathogen *Mycobacterium marinum*

Poornima Mohandas[1,2], William C. Budell[1,2], Emily Mueller[1], Andrew Au[1], Glennon V. Bythrow[1,2] and Luis E. N. Quadri[1,2,*]

[1]Biology Department, Brooklyn College, City University of New York, Brooklyn, NY 11210, USA and [2]Biology Program, Graduate Center, City University of New York, NY 10016, USA

*Corresponding author: Biology Department, Brooklyn College, 2900 Bedford Avenue, Brooklyn, NY 11210, USA. Tel: (718)-951-6254; Fax: (718)-951-4659; E-Mail: LQuadri@brooklyn.cuny.edu

One sentence summary: Analysis of mycobacterial mutants with knockouts in the biosynthetic pathway of PDIM/PGL cell wall (glyco)lipids revealed a complex picture of pleiotropic patterns and uncovered unexpected phenotypic inequalities.

Editor: Sandhya Visweswariah

ABSTRACT

Phthiocerol dimycocerosates (PDIMs) and phenolic glycolipids (PGLs) contribute to the pathogenicity of several mycobacteria. Biosynthesis of these virulence factors requires polyketide synthases and other enzymes that represent potential targets for the development of adjuvant antivirulence drugs. We used six isogenic *Mycobacterium marinum* mutants, each with a different gene knockout in the PDIM/PGL biosynthetic pathway, to probe the pleiotropy of mutations leading to PDIM$^-$ PGL$^-$, PDIM$^+$ PGL$^-$ or PDIM$^-$ PGL$^+$ phenotypes. We evaluated the *M. marinum* mutants for changes in antibiotic susceptibility, cell envelope permeability, biofilm formation, surface properties, sliding motility and virulence in an amoeba model. The analysis also permitted us to begin exploring the hypothesis that different gene knockouts rendering the same PDIM and/or PGL deficiency phenotypes lead to *M. marinum* mutants with equivalent pleiotropic profiles. Overall, the results of our study revealed a complex picture of pleiotropic patterns emerging from different gene knockouts, uncovered unexpected phenotypic inequalities between mutants, and provided new insight into the phenotypic consequences of gene knockouts in the PDIM/PGL biosynthetic pathway.

Keywords: *Mycobacterium*; cell wall biosynthesis; polyketide; amoeba; biofilm; outer membrane lipids

INTRODUCTION

The hallmark of the *Mycobacterium* genus is a unique cell wall that includes an outer membrane-like structure with unusual (glyco)lipids, some of which have been implicated in pathogenesis (Guenin-Mace, Simeone and Demangel 2009; Neyrolles and Guilhot 2011). Phthiocerol dimycocerosates (PDIMs) and phenolic glycolipids (PGLs) are two related families of (glyco)lipids thought to localize to the outer membrane of *M. tuberculosis*, *M. leprae*, and several opportunistic mycobacterial pathogens, including *M. marinum* (*Mmar*) (for a review, see Onwueme *et al*. 2005) (Fig. 1A). These unique (glyco)lipids are involved in pathogenicity through intricate and incompletely
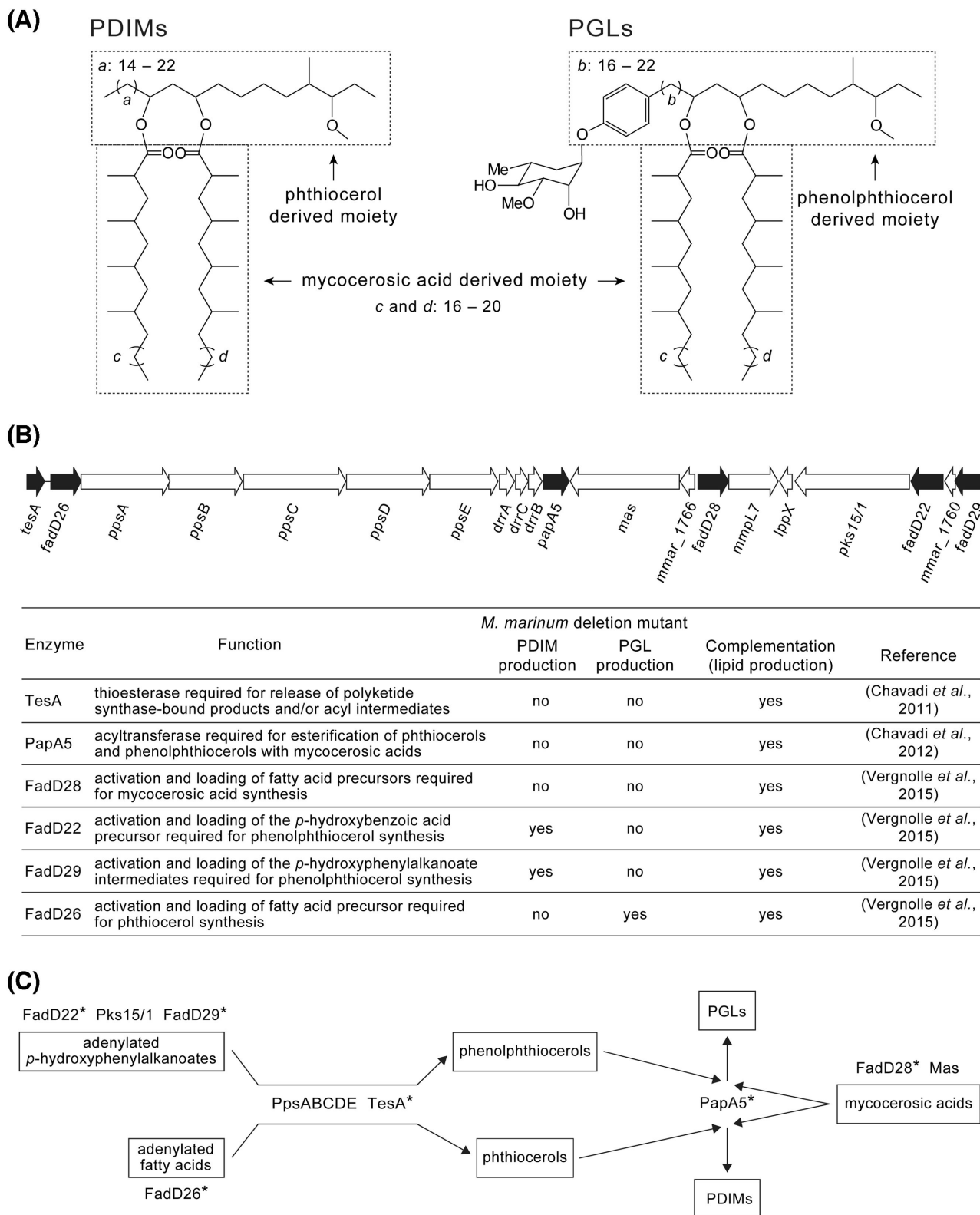
Enzyme	Function	*M. marinum* deletion mutant		Complementation (lipid production)	Reference
		PDIM production	PGL production		
TesA	thioesterase required for release of polyketide synthase-bound products and/or acyl intermediates	no	no	yes	(Chavadi *et al.*, 2011)
PapA5	acyltransferase required for esterification of phthiocerols and phenolphthiocerols with mycocerosic acids	no	no	yes	(Chavadi *et al.*, 2012)
FadD28	activation and loading of fatty acid precursors required for mycocerosic acid synthesis	no	no	yes	(Vergnolle *et al.*, 2015)
FadD22	activation and loading of the *p*-hydroxybenzoic acid precursor required for phenolphthiocerol synthesis	yes	no	yes	(Vergnolle *et al.*, 2015)
FadD29	activation and loading of the *p*-hydroxyphenylalkanoate intermediates required for phenolphthiocerol synthesis	yes	no	yes	(Vergnolle *et al.*, 2015)
FadD26	activation and loading of fatty acid precursor required for phthiocerol synthesis	no	yes	yes	(Vergnolle *et al.*, 2015)

Figure 1. PDIMs, PGLs and chromosomal locus involved in their production. The structures are representative of those produced by *M. marinum* (**A**). The genes deleted in the *M. marinum* isogenic mutants analyzed in this study are highlighted with black-filled arrows (**B**). The roles of the gene products and the previously determined PDIM/PGL phenotype of each deletion mutant and corresponding complemented strain are outlined. The position of the enzymes missing in the mutants (*) in the biosynthetic pathway is schematically depicted (**C**).

understood mechanisms (Arbues *et al.* 2014), and recent studies suggest complementary roles of PDIMs and PGLs in a complex immune evasion mechanism (Cambier *et al.* 2014). There is also evidence that, at least in some species, these lipids strengthen the cell envelope permeability barrier and increase the bacterium's intrinsic antibiotic resistance (Camacho *et al.* 2001; Alibaud *et al.* 2011; Chavadi *et al.* 2011; Yu *et al.* 2012; Soetaert *et al.* 2015).

The relevance of PDIMs and PGLs in mycobacterial biology highlights the enzymes needed for biosynthesis of these virulence factors as attractive targets for exploring the development of adjuvant antivirulence drugs. This consideration has provided thrust for numerous studies that led to the identification of several conserved genes required for PDIM and/or PGL production and the elucidation of the specific roles that many of these genes play in the pathway (for a review, see Quadri 2014). Interestingly, the knowledge gained from some of these studies guided the design of the first PGL biosynthesis inhibitor (Ferreras *et al.* 2008). The inhibitor targets a *p*-hydroxybenzoic acid adenylating enzyme (FadD22) essential for PGL synthesis and has potent activity in *M. tuberculosis* complex members and nontuberculous mycobacterial pathogens, such as *Mmar* (Ferreras *et al.* 2008; He *et al.* 2009). *Mmar*, a close genetic relative of the *M. tuberculosis* complex, causes tuberculosis-like disease in poikilotherms and peripheral granulomatous disease in humans (Cambau and Aubry 2011). Recent studies have shown both PDIMs and PGLs are required for *Mmar* virulence in the zebrafish model (Alibaud *et al.* 2011; Yu *et al.* 2012; Cambier *et al.* 2014).

We have recently reported mutational studies that interrogated the involvement of the *Mmar* genes *tesA*, *papA5*, *fadD22*, *fadD26*, *fadD28* and *fadD29* in the production of PDIMs and PGLs (Chavadi *et al.* 2011, 2012; Vergnolle *et al.* 2015) (Fig. 1B). These six genes are conserved in *M. tuberculosis* and other mycobacteria (Onwueme *et al.* 2005) and their proposed functions in PDIM and/or PGL synthesis are outlined in Fig. 1B (for a review, see Quadri 2014). These studies were based on gene-specific, unmarked deletion mutants and each PDIM and/or PGL deficiency was complemented by episomal expression of a wild-type (WT) copy of the deleted gene, thus permitting unambiguous genotype–phenotype assignments (Fig. 1B). Overall, these findings are in line with those from other reports (Alibaud *et al.* 2011; Yu *et al.* 2012).

In this study, we utilized the *Mmar* isogenic mutants noted above to further interrogate the phenotypic consequences of each of the six gene knockouts. We evaluated the mutants in *in vitro* assays that probed for changes in antibiotic susceptibility, cell envelope permeability, biofilm formation, surface properties and sliding motility. We also explored the virulence of the mutants using the *Dictyostelium discoideum* model. The parallel analysis of these isogenic mutants permitted us to begin exploring the hypothesis that different knockouts in the pathway rendering the same PDIM and/or PGL deficiency lead to mutants with equivalent pleiotropic profiles. Exploration of this hypothesis is relevant in the context of considering specific enzymes of the pathway as potential targets for adjuvant drug development.

MATERIALS AND METHODS

Strains and culturing conditions

Mycobacteria (Table 1) were cultured in Middlebrook 7H9 medium supplemented with 10% ADN (5% BSA, 2% dextrose, 0.85% NaCl), 0.05% Tween-80 and 0.2% glycerol (supplemented 7H9) or Middlebrook 7H11 medium supplemented with 10% ADN and 0.5% glycerol (supplemented 7H11) (Parish and Stoker 1998).

Kanamycin (30 μg mL^{-1}) was added to the media for maintenance of pCP0 plasmids. *Mmar* WT and the *Mmar* mutants carried pCP0 (Ferreras *et al.* 2008), the vector used for episomal complementation. *Dictyostelium discoideum* DH1-10 was axenically cultured under standard conditions in HL5 medium (Eichinger and Rivero 2013).

Antibiotic susceptibility

The studies were conducted using a microdilution method (Chavadi *et al.* 2011). Plates were incubated at 30°C with orbital shaking (170 rpm) for 8 days and growth was assessed by measuring OD$_{595}$ using a plate reader. MIC$_{90}$ values for fold-change determinations were calculated from sigmoidal curves fitted to dose-response datasets using GraphPad Prism (GraphPad Software, Inc., Monroe, North Carolina, United States of America) as reported (Ollinger *et al.* 2013).

Ethidium bromide accumulation

Assay conditions were guided by those published (Yu *et al.* 2012). Briefly, mycobacteria resuspended in 50 mM phosphate-buffered solution, pH 7 (PBS) were loaded into black, flat-bottom, 96-well plates (Greiner Bio-One Co., La Jolla, California, United States of America) at 152 μL per well. Following loading, 8 μL of a 10% glucose solution in PBS and 40 μL of an ethidium bromide (EtBr) solution in PBS (25 mg L^{-1}) were added to the wells and fluorescence intensity (535 nm excitation, 595 nm emission) was kinetically measured for 30 min using a plate reader. EtBr accumulation rates were determined as the slope of the linear regression fitted to datasets of relative fluorescence units versus time.

Biofilm and pellicle formation

MBEC^{TM} plates (Innovotech Inc., Edmonton, Alberta, Canada) were loaded (150 μL per well) with bacterial cultures (10^6 CFU per mL; 7H9 medium with 0.2% glycerol) and incubated (30°C, 100 rpm, 4 weeks) for biofilm formation. Biofilm formation was quantified using a crystal violet colorimetric method (O'Toole 2011) and imaged using an Olympus BX41 microscope (Olympus Corp., Center Valley, Pennsylvania, United States of America). Pellicle formation was investigated using a 24-well plate assay similar to those reported (Pang *et al.* 2012; Tatham *et al.* 2012). Wells preloaded with Sauton's medium (1 mL per well) were surface inoculated with a saturated culture (10 μL) and pellicles were imaged after plate incubation (30°C, 5 weeks).

Sliding motility

The assay was conducted as reported (Tatham *et al.* 2012). Briefly, mycobacterial cultures were spotted (5 μL) on the center of sliding motility plates (7H9 medium, 0.3% or 0.5% agarose, 6% glycerol). Inoculated plates were incubated at 30°C (12 days and 14 days for 0.3% and 0.5% agarose plates, respectively). Sliding motility was determined as the diameter of the spreading colony.

Congo red binding

Plates of supplemented or nonsupplemented 7H11 medium without or with 100 μg mL^{-1} of Congo red (CR) (Tatham *et al.* 2012) were spot-inoculated with 2 μL of cultures grown to saturation. Inoculated plates were incubated at 30°C for 2 weeks (supplemented) or 4 weeks (nonsupplemented). Mycobacterial colonies were imaged using an Olympus SZX7 stereo microscope

Table 1. Mycobacterial strains.

Strain	Characteristics	Reference
M. marinum M (ATCC BAA-535)	Human clinical isolate, wild-type, PDIM$^+$ PGL$^+$	Snapper *et al.* (1990)
M. marinum Δ*fadD22*	*fadD22* (MMAR_1761 / MMAR_RS08725)* deletion, PDIM$^+$ PGL$^-$	Vergnolle *et al.* (2015)
M. marinum Δ*fadD22-c*	*fadD22* deletion, carries a pCP0 vector derivative expressing *fadD22*, PDIM$^+$ PGL$^+$ (complemented strain)	Vergnolle *et al.* (2015)
M. marinum Δ*fadD26*	*fadD26* (MMAR_1777 / MMAR_RS08805) deletion, PDIM$^-$ PGL$^+$	Vergnolle *et al.* (2015)
M. marinum Δ*fadD26-c*	*fadD26* deletion, carries a pCP0 derivative expressing *fadD26*, PDIM$^+$ PGL$^+$ (complemented strain)	Vergnolle *et al.* (2015)
M. marinum Δ*fadD28*	*fadD28* (MMAR_1765 / MMAR_RS08745) deletion, PDIM$^-$ PGL$^-$	Vergnolle *et al.* (2015)
M. marinum Δ*fadD28-c*	*fadD28* deletion, carries a pCP0 derivative expressing *fadD28*, PDIM$^+$ PGL$^+$ (complemented strain)	Vergnolle *et al.* (2015)
M. marinum Δ*fadD29*	*fadD29* (MMAR_1759 / MMAR_RS08715) deletion, PDIM$^+$ PGL$^-$	Vergnolle *et al.* (2015)
M. marinum Δ*fadD29-c*	*fadD29* deletion, carries a pCP0 derivative expressing *fadD29*, PDIM$^+$ PGL$^+$ (complemented strain)	Vergnolle *et al.* (2015)
M. marinum Δ*tesA*	*tesA* (MMAR_1778 / MMAR_RS08810) deletion, PDIM$^-$ PGL$^-$	Chavadi *et al.* (2011)
M. marinum Δ*tesA-c*	*tesA* deletion, carries a pCP0 derivative expressing *tesA*, PDIM$^+$ PGL$^+$ (complemented strain)	Chavadi *et al.* (2011)
M. marinum Δ*papA5*	*papA5* (MMAR_1768 / MMAR_RS08760) deletion, PDIM$^-$ PGL$^-$	Chavadi *et al.* (2012)
M. marinum Δ*papA5-c*	*papA5* deletion, carries a pCP0 derivative expressing *papA5*, PDIM$^+$ PGL$^+$ (complemented strain)	Chavadi *et al.* (2012)
M. smegmatis MC^{2}155 (ATCC 700084)	Nonpathogenic species, lacks the PDIM/PGL biosynthetic pathway	Snapper *et al.* (1990)

*Original and re-annotated locus tag designations as per National Center for Biotechnology Information (NCBI, http://www.ncbi.nlm.nih.gov/) are provided for each gene.

(Olympus Corp., Center Valley, Pennsylvania, United States of America).

Dictyostelium discoideum inhibition

The experiments were performed using a 24-well plate platform and adapted from a recently published assay (Alibaud *et al.* 2011). The inoculum of amoeba cells was expanded from the 100-to-10 000 reported range to a 10-to-150 000 range and escalated using 2-fold increments, as opposed to the 10-fold increments used previously. Plates were incubated for 14 days at 25°C. Starting on the third day, wells were visually inspected for formation of phagocytic plaques daily for 10 days. Amoebal growth was defined for any given set of duplicate wells (same amoeba inoculum) that exhibited at least two plaques in each well.

RESULTS AND DISCUSSION

Different gene knockouts in the PDIM/PGL biosynthetic pathway increase antibiotic susceptibility and weaken the cell envelope permeability barrier by different magnitudes

Recent studies in *Mmar* indicated that disruption of *tesA*, *fadD28* or *fadD26* produces antibiotic hypersusceptibility (Alibaud *et al.* 2011; Chavadi *et al.* 2011; Yu *et al.* 2012) and that disruption of *fadD28* or *fadD26* increases cell envelope permeability, as judged by dye accumulation assays (Yu *et al.* 2012). These studies support the notion that loss of PDIMs leads to antibiotic hypersusceptibility and increased cell envelope permeability, but provide no information as to whether selective loss of PGLs affects these phenotypic traits as well. To address this knowledge gap and expand our understanding of the phenotypic consequences of

inactivating different genes required for PDIM and/or PGL production, we tested the susceptibility of our six *Mmar* mutants to antibiotics of different classes. In addition, we investigated the EtBr accumulation rates in the mutants to probe for changes in cell envelope permeability.

In the susceptibility experiments, the group of antibiotics tested included rifampicin, doxycycline, ciprofloxacin and streptomycin, which are used in the treatment of *Mmar* infections (Rallis and Koumantaki-Mathioudaki 2007). A strain was defined as having altered susceptibility when it displayed >2-fold change in MIC$_{90}$ value relative to WT. As per this criterion, each mutant showed hypersusceptibility to at least one of the six antibiotics tested, while none of the mutants displayed reduced susceptibility to any of these antibiotics (Fig. 2A). The *tesA* and *papA5* mutants showed qualitatively and quantitatively comparable hypersusceptibility profiles (Fig. 2A). The profiles of the remaining mutants were, for the most part, qualitatively comparable, yet quantitatively attenuated relative to that of the *tesA* and *papA5* mutants (Fig. 2A). The susceptibility changes appears to be antibiotic-specific and uncorrelated with antibiotic lipophilicity (e.g. log *P* (Kerns and Di 2008)). Episomal expression in the mutants of a WT copy of the deleted gene flattened the hypersusceptibility profiles (Fig. 2B). Notably, the attenuated hypersusceptibility profile of the *fadD28* mutant is unexpected because the mutant shares the PDIM$^-$ PGL$^-$ phenotype with the *tesA* and *papA5* mutants and has an increase in envelope permeability comparable to that of these mutants (See below). The reason for this phenotypic inequality is unclear. Perhaps production of anomalous lipid variants with surrogate acyl chains in the absence of mycocerosic acids due to *fadD28* deletion in *Mmar* Δ*fadD28* is responsible for the unexpected phenotypic profile. Appearance of anomalous PDIM-like variants with abnormal acyl chains has been documented in the mycocerosic
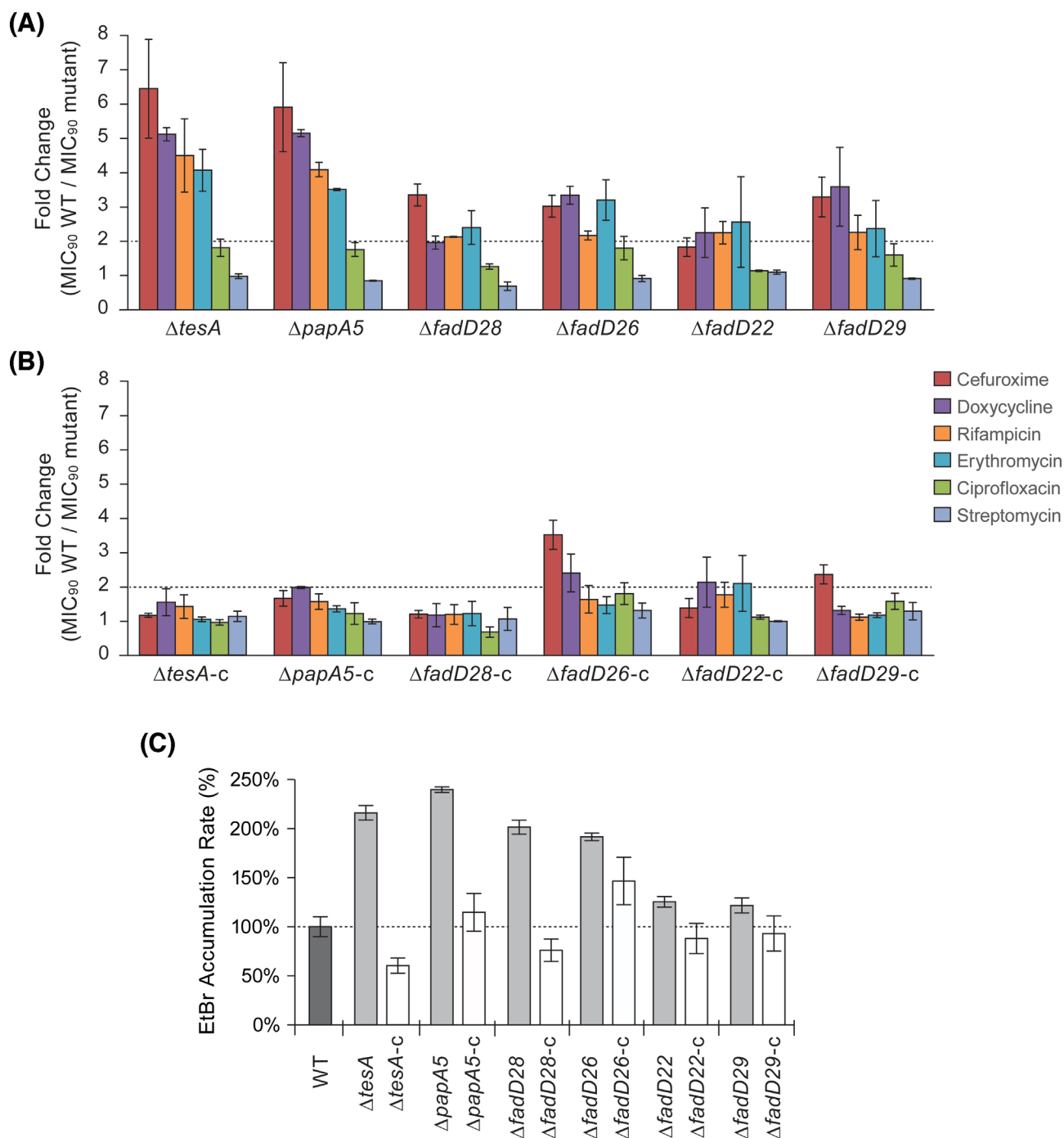
Figure 2. Antibiotic susceptibility and ethidium bromide accumulation rate of *M. marinum* strains. Fold-change in MIC$_{90}$ values between the WT strain and the mutants **(A)** or the mutants constitutively expressing an episomal WT copy of the deleted gene **(B)** are shown. A strain was defined as having an altered antibiotic susceptibility when it displayed >2-fold change (dotted line) relative to WT. The antimicrobial susceptibility results represent means and SEM of three independent experiments. The ethidium bromide (EtBr) accumulation data **(C)** correspond to means and SEM of five independent experiments.

acid-deficient mutant of *M. bovis* BCG (Azad *et al.* 1996; Fitzmaurice and Kolattukudy 1998).

The six gene knockouts also correlated with an increase in EtBr accumulation rate, a reporter of cell envelope permeability barrier integrity (Fig. 2C). Knockouts leading to concurrent loss of PDIMs and PGLs or selective loss of PDIMs roughly doubled the rate of EtBr accumulation, whereas knockouts selectively eliminating PGLs produced only a 25% increase. Many factors are likely to influence the antibiotic susceptibility of each mutant to individual antibiotics, including differences in

drug uptake and/or efflux. The weakening of the permeability barrier might also affect the antibiotic susceptibility of the mutants by permitting better antibiotic penetration. However, the pattern of changes of EtBr accumulation rate (Fig. 2C) and antibiotic susceptibility (Fig. 2A) do not fully correlate across mutants. Taken together, the results indicate that only two out of the three knockouts producing concurrent loss of PDIMs and PGLs lead to a marked increase in susceptibility to specific antibiotics and that mutations resulting in selective loss of PDIMs or PGLs affect antibiotic susceptibility to a lesser degree. The results also
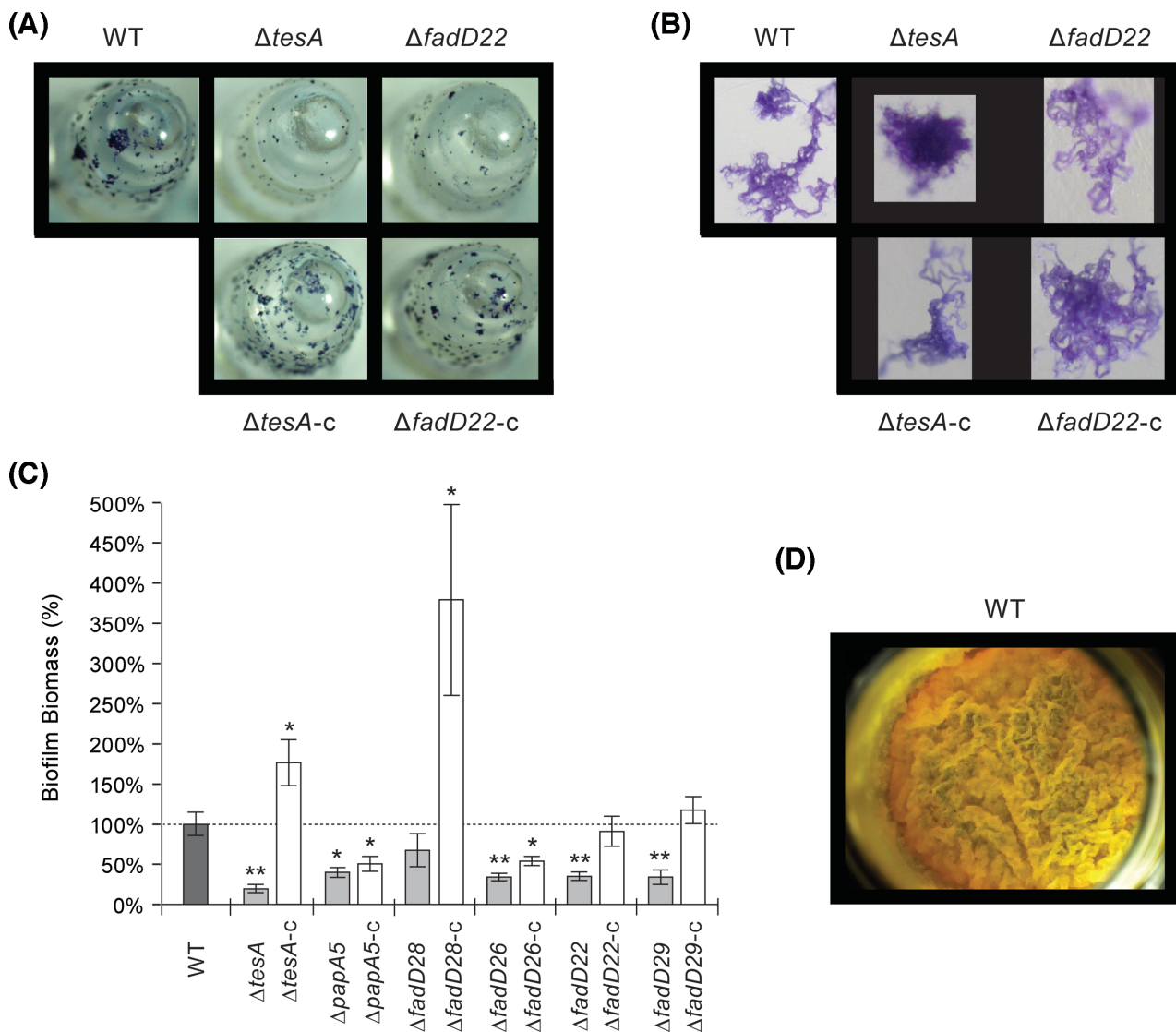
Figure 3. Biofilm formation by *M. marinum* strains. Representative peg (**A**) and biofilm microcolony (**B**) images of the WT, two mutants (one PDIM⁻ PGL⁻ and one PDIM⁺ PGL⁻), and corresponding genetically complemented strains are shown. The results with these mutants are comparable to those seen with the rest of the mutants. Biofilm formation on the pegs was quantified using a standard colorimetric method (**C**). The results represent means and SEM of a minimum of six independent experiments. Student's *t*-test *p* values versus WT: *, <0.05; **, <0.01. All strains formed comparable pellicles on the surface of the liquid growth medium (**D**). The representative pellicle shown is for the WT.

suggest that PDIMs have a more significant role than PGLs in the integrity of the cell envelope permeability barrier.

Gene knockouts in the PDIM/PGL biosynthetic pathway are detrimental to biofilm formation and affect cell surface properties but not sliding motility

Recent studies have implicated the production of *Mmar* cell wall glycolipids known as lipooligosaccharides in biofilm formation and sliding motility (Ren *et al.* 2007). Loss of lipooligosaccharide production also leads to increased binding of the hydrophobic dye CR, a marker of cell envelope hydrophobicity (Etienne *et al.* 2009). These observations raise the possibility that other cell wall (glyco)lipids of *Mmar* might be relevant for these phenotypic traits. To our knowledge, the effect of PDIM or PGL production on biofilm formation, sliding motility and CR binding has not been reported. Thus, we explored these phenotypic traits in the *Mmar*

mutants and expanded the study to assess the effect of the gene knockouts on pellicle formation (biofilm-type growth on a liquid surface) as well.

As expected, the WT formed biofilms on the pegs of the MBEC device (Fig. 3A) and its biofilm microcolonies displayed the characteristic serpentine cords (Fig. 3B) (Ceri *et al.* 1999; Hall-Stoodley *et al.* 2006). The mutants exhibited smaller and/or less abundant microcolonies (Fig. 3A) and less biofilm formation overall (32%–80% reduction relative to WT) (Fig. 3C). The *tesA*, *papA5* and *fadD26* mutants (all sharing loss of PDIMs) had more compact cell aggregates and less cording than WT (Fig. 3B). On the other hand, the microcolonies of the *fadD28* mutant retained the WT phenotype (not shown). Thus, as seen in the antibiotic susceptibility experiments, the phenotype of the *fadD28* mutant unexpectedly deviated from that of the other two PDIM⁻ PGL⁻ mutants (*tesA* and *papA5*). Episomal expression in the mutants of a WT copy of the deleted gene tended to increase biofilm formation and corrected the cording deficiency.
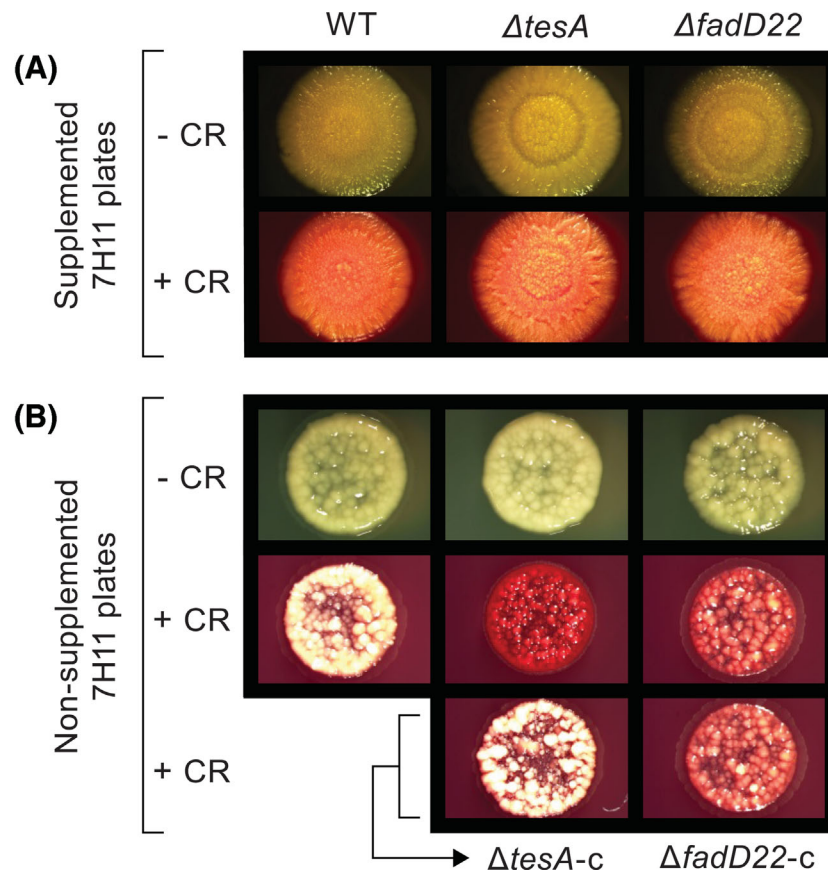
Figure 4. CR binding properties of *M. marinum* strains. Plates of supplemented or nonsupplemented medium without or with CR were spot-inoculated with *M. marinum* cultures, incubated for growth, and imaged. Images of the WT, two mutants (one PDIM⁻ PGL⁻ and one PDIM⁺ PGL⁻), and corresponding genetically complemented strains are shown. The results shown for these mutants are comparable to those seen with the rest of the mutants, except by the complementation differences noted in the text. The data is representative of three independent experiments.

The WT and the mutants had an equally robust pellicle formation capacity and their pellicles showed a comparably rich surface topology with folds, ridges and creases (Fig. 3D). There was no significant difference in sliding motility between the WT and the mutants either (Student's *t*-test *P* values > 0.05, *n* = 3; data not shown). On supplemented 7H11 plates, the WT and the mutants developed the same reddish coloration in the presence of CR (Fig. 4A). In contrast, the mutants displayed a drastic increase in CR staining relative to WT on nonsupplemented 7H11 plates (Fig. 4B). Episomal expression in the mutants of a WT copy of the deleted gene led to reversion to WT CR staining only in the *tesA* and *fadD28* mutants, despite the fact that all the genetically complemented mutants regained PDIM and/or PGL production capacity (Fig. 1C) (Chavadi *et al.* 2011, 2012; Vergnolle *et al.* 2015). Taken together, our findings indicate that loss of PDIMs and/or PGLs affect biofilm formation and CR binding (in a medium composition-dependent manner), but do not compromise pellicle formation or sliding motility. To our knowledge, this is the first study indicating that loss of PDIMs and/or PGLs affects biofilm formation.

Different gene knockouts in the PDIM/PGL biosynthetic pathway lead to different attenuation levels in an amoeba model

The phagocytic amoeba *D. discoideum* is a commonly used model to study virulence of mycobacteria and other pathogens (Tosetti,
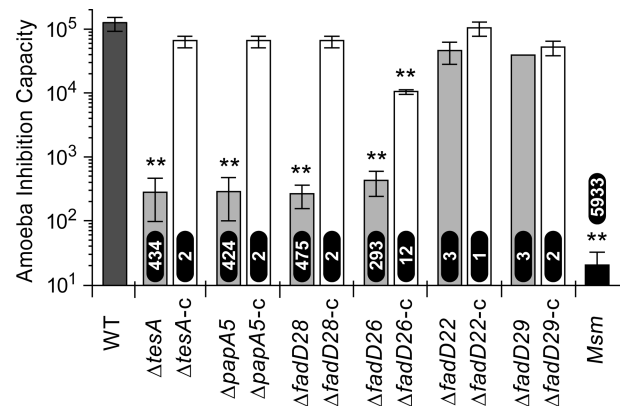

Figure 5. Inhibition of *D. discoideum* by *M. marinum* strains. The virulence of the *M. marinum* strains was comparatively assessed using a *D. discoideum* inhibition assay. In this assay, the highest amoeba inoculum inhibited by each strain is considered a measure of its virulence. The fold reduction in virulence of each strain relative to *M. marinum* WT is shown at the base of each bar for the mutants and above the bar for *M. smegmatis* (*Msm*). The results correspond to means and SEM of three experiments. **, Student's *t*-test *P* < 0.01 (versus WT).

Croxatto and Greub 2014). Mycobacterial pathogens such as *Mmar* multiply intracellularly in permissive endosomal compartments and produce amoebal growth inhibition (Hagedorn and Soldati 2007; Kennedy, Morisaki and Champion 2012). We probed the virulence of the *Mmar* mutants (Fig. 5) using a

D. discoideum inhibition assay in which a *Mmar tesA* transposon mutant previously showed attenuation (Alibaud *et al.* 2011). We found a drastic reduction in virulence (∼300-fold–∼500-fold relative to WT) for the *tesA*, *papA5*, *fadD28* and *fadD26* mutants. On the other hand, the *fadD22* and *fadD29* mutants exhibited a modest virulence reduction (3-fold). Episomal expression of a WT copy of the deleted gene increased the virulence of the mutants (Fig. 5). Our results indicate that concurrent loss of PDIMs and PGLs or selective loss of PDIMs leads to severe attenuation in the *D. discoideum* model. In contrast, selective loss of PGLs is relatively inconsequential in this model. These findings support the view that PDIMs have a more critical role than PGLs in the pathogenicity of *Mmar* against *D. discoideum*. In *M. tuberculosis*, disruption of *fadD28* impairs the ability of the pathogen to arrest phagolysosome maturation (Brodin *et al.* 2010), possibly by the lack of PDIMs to elicit pathogen-directed reorganization of host membrane lipids (Astarie-Dequeker *et al.* 2009). This precedent highlights the possibility that the attenuation of the *Mmar* mutants might emerge from a reduced capacity to arrest the amoebal phagolysosome maturation pathway and create protective niches. Interestingly, even the most attenuated mutant remained significantly more virulent than the nonpathogenic *M. smegmatis*. This suggests that *Mmar* has multiple virulence factors contributing to its interplay with the amoeba. This notion is not surprising considering that *Mmar* and amoebae share environmental niches and that amoebae are thought to act as evolutionary training grounds for intracellular bacterial pathogens (Molmeret *et al.* 2005).

CONCLUSIONS

Our findings provide new insight into the consequences (or lack thereof) of different knockouts in the PDIM/PGL biosynthetic pathway on various phenotypic traits. The complex pleiotropic patterns arising from the different knockouts might be influenced by changes in metabolic flux redirecting different biosynthetic precursor surpluses to production of other (glyco)lipids (Jain *et al.* 2007; Ferreras *et al.* 2008; Lee *et al.* 2013). Accumulation of different biosynthetic intermediates, some of which might be repurposed for the production of unusual (glyco)lipids with potential phenotypic impacts (Azad *et al.* 1996; Fitzmaurice and Kolattukudy 1998), might also contribute to define the pleiotropic patterns of the mutants seen here. (Glyco)lipidomic profiling will be needed to investigate these possibilities and assist the unraveling of the molecular mechanisms underlying the phenotypic profiles of the mutants. The parallel analysis of isogenic mutants reported herein permitted us to uncover unexpected phenotypic inequalities. Most noticeably, the differences in antibiotic susceptibility and microcolony morphology between the *tesA* (or *papA5*) and *fadD28* knockouts (both leading to a PDIM⁻ PGL⁻ phenotype) suggest that the enzymes encoded by these genes might not be equivalent targets for adjuvant drug development. In more general terms, our findings advocate that the notion that different enzymes of a metabolic pathway for which elimination equally leads to pathway shutdown are equivalent potential targets for drug development might not always hold true.

ACKNOWLEDGEMENTS

FUNDING

REFERENCES

Alibaud L, Rombouts Y, Trivelli X *et al*. A *Mycobacterium marinum* TesA mutant defective for major cell wall-associated lipids is highly attenuated in *Dictyostelium discoideum* and zebrafish embryos. *Mol Microbiol* 2011;**80**:919–34.

Arbues A, Lugo-Villarino G, Neyrolles O *et al*. Playing hide-and-seek with host macrophages through the use of mycobacterial cell envelope phthiocerol dimycocerosates and phenolic glycolipids. *Front Cell Infect Microbiol* 2014;**4**:173.

Astarie-Dequeker C, Le Guyader L, Malaga W *et al*. Phthiocerol dimycocerosates of *M. tuberculosis* participate in macrophage invasion by inducing changes in the organization of plasma membrane lipids. *PLoS Pathog* 2009;**5**:e1000289.

Azad AK, Sirakova TD, Rogers LM *et al*. Targeted replacement of the mycocerosic acid synthase gene in *Mycobacterium bovis* BCG produces a mutant that lacks mycosides. *P Natl Acad Sci USA* 1996;**93**:4787–92.

Brodin P, Poquet Y, Levillain F *et al*. High content phenotypic cell-based visual screen identifies *Mycobacterium tuberculosis* acyltrehalose-containing glycolipids involved in phagosome remodeling. *PLoS Pathog* 2010;**6**:e1001100.

Camacho LR, Constant P, Raynaud C *et al*. Analysis of the phthiocerol dimycocerosate locus of *Mycobacterium tuberculosis*. Evidence that this lipid is involved in the cell wall permeability barrier. *J Biol Chem* 2001;**276**:19845–54.

Cambau E, Aubry A. *Mycobacterium marinum*. In: Schlossberg D (ed). *Tuberculosis and Nontuberculous Mycobacterial Infections*. Herndon, VA: ASM Press, 2011, 586–600.

Cambier CJ, Takaki KK, Larson RP *et al*. Mycobacteria manipulate macrophage recruitment through coordinated use of membrane lipids. *Nature* 2014;**505**:218–22.

Ceri H, Olson ME, Stremick C *et al*. The calgary biofilm device: new technology for rapid determination of antibiotic susceptibilities of bacterial biofilms. *J Clin Microbiol* 1999;**37**:1771–6.

Chavadi S, Onwueme K, Edupuganti U *et al*. The mycobacterial acyltransferase PapA5 is required for biosynthesis of cell wall-associated phenolic glycolipids. *Microbiology* 2012;**158**:1379–87.

Chavadi SS, Edupuganti UR, Vergnolle O *et al*. Inactivation of *tesA* reduces cell wall lipid production and increases drug susceptibility in mycobacteria. *J Biol Chem* 2011;**286**:24616–25.

Eichinger L, Rivero F. *Dictyostelium Discoideum Protocols*. Springer Verlag, Heidelberg, Germany: Humana Press, 2013.

Etienne G, Malaga W, Laval F *et al*. Identification of the polyketide synthase involved in the biosynthesis of the surface-exposed lipooligosaccharides in mycobacteria. *J Bacteriol* 2009;**191**:2613–21.

Ferreras JA, Stirrett KL, Lu X *et al*. Mycobacterial phenolic glycolipid virulence factor biosynthesis: mechanism and small-molecule inhibition of polyketide chain initiation. *Chem Biol* 2008;**15**:51–61.

Fitzmaurice AM, Kolattukudy PE. An acyl-CoA synthase (*acoas*) gene adjacent to the mycocerosic acid synthase (*mas*)

locus is necessary for mycocerosyl lipid synthesis in *Mycobacterium tuberculosis* var. *bovis* BCG. *J Biol Chem* 1998;**273**: 8033–9.

Guenin-Mace L, Simeone R, Demangel C. Lipids of pathogenic mycobacteria: contributions to virulence and host immune suppression. *Transbound Emerg Dis* 2009;**56**:255–68.

Hagedorn M, Soldati T. Flotillin and RacH modulate the intracellular immunity of *Dictyostelium* to *Mycobacterium marinum* infection. *Cell Microbiol* 2007;**9**:2716–33.

Hall-Stoodley L, Brun OS, Polshyna G *et al. Mycobacterium marinum* biofilm formation reveals cording morphology. *FEMS Microbiol Lett* 2006;**257**:43–9.

He W, Soll CE, Chavadi SS *et al.* Cooperation between a coenzyme A-independent stand-alone initiation module and an iterative type I polyketide synthase during synthesis of mycobacterial phenolic glycolipids. *J Am Chem Soc* 2009;**131**: 16744–50.

Jain M, Petzold CJ, Schelle MW *et al.* Lipidomics reveals control of *Mycobacterium tuberculosis* virulence lipids via metabolic coupling. *P Natl Acad Sci USA* 2007;**104**:5133–8.

Kennedy GM, Morisaki JH, Champion PA. Conserved mechanisms of *Mycobacterium marinum* pathogenesis within the environmental amoeba *Acanthamoeba castellanii. Appl Environ Microb* 2012;**78**:2049–52.

Kerns EH, Di L. Lipophilicity. In: Kerns EH, Di L (eds). *Drug-Like Properties: Concepts, Structure Design and Methods: From ADME to Toxicity Optimization.* San Diego: Academic Press, 2008, 43–7.

Lee W, VanderVen BC, Fahey RJ *et al.* Intracellular *Mycobacterium tuberculosis* exploits host-derived fatty acids to limit metabolic stress. *J Biol Chem* 2013;**288**:6788–800.

Molmeret M, Horn M, Wagner M *et al.* Amoebae as training grounds for intracellular bacterial pathogens. *Appl Environ Microb* 2005;**71**:20–8.

Neyrolles O, Guilhot C. Recent advances in deciphering the contribution of *Mycobacterium tuberculosis* lipids to pathogenesis. *Tuberculosis (Edinb)* 2011;**91**:187–95.

O'Toole GA. Microtiter dish biofilm formation assay. *J Vis Exp* 2011;**47**:e2437.

Ollinger J, Bailey MA, Moraski GC *et al.* A dual read-out assay to evaluate the potency of compounds active against *Mycobacterium tuberculosis. PLoS One* 2013;**8**:e60531.

Onwueme KC, Vos CJ, Zurita J *et al.* The dimycocerosate ester polyketide virulence factors of mycobacteria. *Prog Lipid Res* 2005;**44**:259–302.

Pang JM, Layre E, Sweet L *et al.* The polyketide Pks1 contributes to biofilm formation in *Mycobacterium tuberculosis. J Bacteriol* 2012;**194**:715–21.

Parish T, Stoker NG, Walker JM (eds). General culture methodology and safety considerations. *Mycobacteria Protocols*, Vol. 101. Totowa, New Jersey: Humana Press, 1998, 15–30.

Quadri LE. Biosynthesis of mycobacterial lipids by polyketide synthases and beyond. *Crit Rev Biochem Mol* 2014;**49**:179–211.

Rallis E, Koumantaki-Mathioudaki E. Treatment of *Mycobacterium marinum* cutaneous infections. *Expert Opin Pharmaco* 2007;**8**:2965–7298.

Ren H, Dover LG, Islam ST *et al.* Identification of the lipooligosaccharide biosynthetic gene cluster from *Mycobacterium marinum. Mol Microbiol* 2007;**63**:1345–59.

Snapper SB, Melton RE, Mustafa S *et al.* Isolation and characterization of efficient plasmid transformation mutants of *Mycobacterium smegmatis. Mol Microbiol* 1990;**4**:1911–9.

Soetaert K, Rens C, Wang XM *et al.* Increased vancomycin susceptibility in Mycobacteria: a new approach to identify synergistic activity against multidrug-resistant Mycobacteria. *Antimicrob Agents Ch* 2015;**59**:5057–60.

Tatham E, Chavadi S, Mohandas P *et al.* Production of mycobacterial cell wall glycopeptidolipids requires a member of the MbtH-like protein family. *BMC Microbiol* 2012;**12**:118.

Tosetti N, Croxatto A, Greub G. Amoebae as a tool to isolate new bacterial species, to discover new virulence factors and to study the host-pathogen interactions. *Microb Pathogenesis* 2014;**77**:125–30.

Vergnolle O, Chavadi SS, Edupuganti UR *et al.* Biosynthesis of cell-envelope-associated phenolic glycolipids in *Mycobacterium marinum. J Bacteriol* 2015;**197**:1040–50.

Yu J, Tran V, Li M *et al.* Both phthiocerol dimycocerosates and phenolic glycolipids are required for virulence of *Mycobacterium marinum. Infect Immun* 2012;**80**:1381–9.